Received: 8 August 2023 | Accepted: 3 October 2023

DOI: 10.1002/biof.2022

RESEARCH ARTICLE

Biofactors WILEY

Glycosaminoglycan dermatan sulfate supplementation decreases diet-induced obesity and metabolic dysfunction in mice

Bojan Stojnić[1,2] | **Sebastiá Galmés**[1,3,4] | **Alba Serrano**[1] | **Maria Sulli**[2] | **Lana Sušak**[1] | **Ndioba Seye**[1] | **Andreu Palou**[1,3,4] | **Gianfranco Diretto**[2] | **M. Luisa Bonet**[1,3,4] | **Joan Ribot**[1,3,4]

[1]Laboratory of Molecular Biology, Nutrition, and Biotechnology (Group of Nutrigenomics, Biomarkers and Risk Evaluation), University of the Balearic Islands (UIB), Palma, Spain

[2]Italian National Agency for New Technologies, Energy and Sustainable Development (ENEA), Laboratory Biotechnology, Roma, Italy

[3]Health Research Institute of the Balearic Islands (IdISBa), Palma, Spain

[4]CIBER de Fisiopatología de la Obesidad y Nutrición (CIBERobn), Palma, Spain

Correspondence
M. Luisa Bonet, Laboratory of Molecular Biology, Nutrition, and Biotechnology (Group of Nutrigenomics, Biomarkers and Risk Evaluation), University of the Balearic Islands (UIB), Palma, Spain.
Email: luisabonet@uib.es

Funding information
Agencia Estatal de Investigación, Grant/Award Numbers: AGL2015-67019-P, PGC2018-097436-B-I00

Abstract

Glycosaminoglycans are complex carbohydrates used as nutraceuticals for diverse applications. We studied the potential of the glycosaminoglycan dermatan sulfate (DS) to counteract the development of diet-induced obesity (DIO) using obesity-prone mice fed a high-fat diet (HFD) as a model. Oral DS supplementation protected the animals against HFD-induced increases in whole-body adiposity, visceral fat mass, adipocyte size, blood glucose levels, insulin resistance, and pro-inflammatory lipids levels in brown adipose tissue (BAT) and the liver, where it largely counteracted the HFD-induced changes in the nonpolar metabolome. Protection against DIO in the DS-supplemented mice occurred despite higher energy intake and appeared to be associated with increased energy expenditure, higher uncoupling protein 1 expression in BAT, decreased BAT "whitening," and an enhanced channeling of fuel substrates toward skeletal muscle. This work is the first preclinical study to examine the anti-obesity activity of DS tested individually in vivo. The results support possible uses of DS as an active component in functional foods/supplements to manage obesity and associated metabolic diseases.

KEYWORDS

brown adipose tissue "whitening", functional foods, glycosaminoglycan, nonpolar metabolomics, obesity, skeletal muscle, substrate partitioning

Abbreviations: BAT, brown adipose tissue; DIO, diet-induced obesity; DS, dermatan sulfate; ECM, extracellular matrix; GAG, glycosaminoglycan; HFD, high-fat diet; HOMA-IR, homeostatic model assessment for insulin resistance; MEF, mouse embryo fibroblasts; NEFA, nonesterified fatty acids; NFD, normal-fat diet; PC, phosphatidylcholine; R-QUICKI, revised quantitative insulin sensitivity check index; SM, sphingomyelin; TAG, triacylglycerol; WAT, white adipose tissue.

Bojan Stojnić and Sebastiá Galmés contributed equally to this study and shared the first authorship.

1 | INTRODUCTION

Glycosaminoglycans (GAGs) are complex heteropolysaccharides that serve structural and regulatory functions in animal tissues and are found in foods of animal origin.[1] Chemically, GAGs are linear polymers formed by a repeating disaccharide unit composed of an amino sugar and an uronic acid. Four main classes of GAGs are recognized: chondroitin sulfate or dermatan sulfate (DS), heparan sulfate or heparin, keratan sulfate, and hyaluronic acid.[2] GAGs are components of the cell surface glycocalyx and the extracellular matrix (ECM) of connective and other animal tissues, either in free form (as for hyaluronic acid) or as part of proteoglycans. The latter consists of a core protein with one or more covalently attached sulfated GAG chains making up most of the proteoglycan mass. GAGs/proteoglycans in the ECM interact with many ligands, including growth factors, cytokines and chemokines, cell surface receptors, cell adhesion molecules, and other ECM components, and, by so doing, influence cell fate (e.g., growth, differentiation, migration), cell metabolism and inflammatory responses.[3]

GAGs are used as nutraceuticals for diverse applications,[4] and their potential as anti-obesity agents is under investigation. Preclinical studies have shown high-fat diet (HFD)-induced fat accretion and related metabolic dysfunctions to be attenuated in animals supplemented with GAGs/proteoglycans, such as chondroitin sulfate from salmon cartilage[5] or sea cucumber,[6] proteoglycan from salmon cartilage,[7] and GAGs extracted from certain insects[8,9] and fish waste.[10] The anti-obesity activity of GAGS in those studies was ascribed or related to decreased intestinal fat digestion and absorption,[5,10] increased fecal bile acid excretion,[10] increased sensitization to insulin in the liver,[6] improved leptin response to fasting/refeeding,[7] and decreased hepatic lipogenic capacity.[10,7]

Anti-obesity activity may also arise from effects on adipose tissues since changes in adipose cells' fate and metabolism can affect whole-body energy expenditure, adiposity, and metabolic health. Whereas typical white adipocytes specialize in energy storage and release, brown and beige adipocytes, when active, inefficiently oxidize lipid and glucose fuel substrates to produce heat. Brown and beige adipocytes do so thanks to their shared high mitochondrial oxidative capacity and inducible uncoupling protein 1 (UCP1) expression. Brown adipocytes are found in discrete brown adipose tissue (BAT) depots, while beige adipocytes emerge in white adipose tissue (WAT) depots via browning. BAT activation and WAT browning can oppose obesity, diabetes, and dyslipidemia.[11] However, both BAT and browned WAT can undergo a "whitening" effect, common in obesity and aging, whereby the cell loses the characteristics of a brown adipocyte and assumes those of a white adipocyte.[12,13]

We previously reported that a mix of hyaluronic acid and DS (1:0.25, w/w) contained in a commercially available GAG mix (Oralvisc) synergistically suppressed spontaneous and hormonally-induced adipogenic differentiation of multipotent mouse embryo fibroblasts (MEFs) while favoring chondrogenic differentiation.[14] Suppressive effects on adipogenesis were subsequently reported for GAGs isolated from bovine milk[15] and fish waste[10] in the 3T3-L1 adipocyte cell model. In mice, oral supplementation of the Oralvisc GAG mix enhanced systemic insulin sensitivity and potentiated and accelerated body fat loss during the reversal of diet-induced obesity (DIO), which was associated with an increase in the capacity for mitochondrial oxidative metabolism in visceral WAT.[16] Interestingly, when individually assayed, the minor component of the mix, DS, favored the expression of brown adipocyte marker genes during the adipogenic differentiation of MEFs.[14] DS, also known as chondroitin sulfate-B, is a polymer of sulfated *N*-acetyl-galactosamine and iduronic acid disaccharide unit repeats. In the present study, we aimed to get further insight into the in vivo anti-obesity properties and potential mechanisms of action of DS supplementation by studying its ability to counteract the development of DIO and its effects on metabolism in adipose tissues and other critical homeostatic tissues.

2 | EXPERIMENTAL PROCEDURES

2.1 | Animal experiment

The protocols used were reviewed and approved by the Bioethical Committee of the University of the Balearic Islands (Resolution number CEEA 43/07/15). The use, accommodation, and care of laboratory animals followed EU Directive 2010/63/EU for animal experiments. Animals (three per cage) were housed under standard conditions of controlled temperature (22°C), a 12-h light–dark cycle (light on from 8:00 a.m. to 8:00 h p.m.), and free access to food and tap water.

Twenty-seven 7-week-old C57BL/6J male mice (Jackson Laboratory, Maine, USA) pre-habituated to a defined normal-fat diet (NFD, 10% energy as fat) for 1 week were used. While still on the NFD, one group of animals ($n = 9$) started receiving the DS supplement (30 mg/kg animal/day in 20 μl) orally, through a pipette, roughly at the same hour (between 10:00 a.m. and 11:00 h a.m.) and ensuring complete ingestion; the rest of the animals received placebo (a mix of water and olive oil, used as a vehicle for the DS). After 1-week pretreatment, the DS-treated animals and half of the placebo-treated

animals were challenged with a defined HFD (45% energy as fat) for 4 weeks while continuing to receive the same daily treatments, making out the HF control (non-supplemented) group and the DS group; the remaining placebo-treated animals continued on the NFD and receiving placebo daily during the entire experimental period, making out the NF control group. Diets were obtained from Research Diets (New Brunswick, USA; NFD D12450J and HFD D12451). DS (90% purity, derived from porcine mucosa of healthy pigs, code F0901) was a generous gift from Bioiberica (Palafolls, Barcelona, Spain).

Body weight and food intake were recorded twice a week from the beginning of the treatment until sacrifice. Body weight gain at specific time points was calculated as the difference between the actual and initial body weights and expressed as grams. Cumulative energy intake was estimated per cage from the amount of food consumed and its caloric equivalence and expressed relative to body weight (as kJ/g body weight). Body composition was analyzed immediately before the HFD/NFD challenge and on the fourth week of it, using an Echo MRI-700 body composition analyzer (Echo Medical Systems LLC, Houston, USA). On the fourth week of the HFD/NFD challenge, internal body temperature was also measured—using a calibrated thermometer (RS 612–849; RS, Madrid, Spain) that was gently inserted in the rectum, with Vaseline as lubricant—and a 6-h fast (from 06:00 a.m. to 12:00 a.m.) was applied, after which tail-blood was collected for the assessment of insulin resistance and sensitivity.

The animals were euthanized after 30 days of dietary challenge, by decapitation, under fed conditions, and within the first 2 h of the light cycle. Blood collected from the neck was used to prepare serum, stored at −20°C. Tissues collected included interscapular BAT, inguinal, epididymal, and retroperitoneal WAT (iWAT, eWAT, and rWAT, respectively), gastrocnemius skeletal muscle, and liver. Tissues were dissected in their entirety, weighed, snap-frozen in liquid nitrogen, and stored at −80°C until processed. Samples of iWAT and BAT were fixed for subsequent histological studies. The sum of the mass of all collected WAT depots expressed as a percentage of body weight was taken as the adiposity index, and the ratio between the sum of the masses of eWAT and rWAT divided by the mass of iWAT, as the visceral to subcutaneous fat ratio. The liver mass expressed as a percentage of body weight was taken as the liver index.

2.2 | Blood parameters and surrogate indexes of insulin resistance and sensitivity

Blood glucose levels were determined using an Accu-Chek Aviva system (Roche Diagnostics, Risch, Switzerland). Commercial kits were used to measure serum insulin (Mercodia, Uppsala, Sweden) and nonesterified fatty acids (NEFA; Wako Chemicals GmbH, Neuss, Germany), following the manufacturer's protocols. Insulin resistance and insulin sensitivity indexes were derived from basal glucose, insulin, and NEFA levels in plasma after a 6-h fast. The homeostatic model assessment for insulin resistance (HOMA-IR) score was calculated as HOMA-IR = [insulin (μU/l) × glucose (mmol/l)/22.5],[17] and the revised quantitative insulin sensitivity check index (R-QUICKI) as R-QUICKI = 1/[log glucose (mg/dl) + log insulin (μU/ml) + log NEFA (mM/l)].[18]

2.3 | Liver total lipid content

Total hepatic lipids were extracted from 50 to 100 mg of tissue as described.[19] Lipid content per gram of tissue was calculated from the weight of the tubes following evaporation of the final hexane extract, subtracting the initial (clean) tube weight and considering the initial amount of tissue used.

2.4 | RNA isolation, retrotranscription, and real-time PCR

Total RNA was extracted from tissue samples using commercial E.Z.N.A. Total RNA kit I (Omega Bio-Tek, Georgia, USA), following the supplier's instructions. Isolated RNA was quantified using a Nanodrop ND 1000 spectrophotometer (Nano-Drop Technologies Inc., Wilmington, USA), and its integrity was confirmed by agarose gel electrophoresis. Reverse transcription, PCR amplification of selected cDNAs, and data analysis were conducted as described.[20] The sequences of the primers used (from Sigma-Aldrich, Madrid, Spain) are available upon request. Data were normalized against beta-actin as the reference.

2.5 | Immunoblotting

BAT tissue homogenization, measurement of total protein content, separation of proteins by SDS-polyacrylamide gel electrophoresis, and blotting to nitrocellulose membrane were performed as detailed previously.[21] Blocked membranes were successively probed for up to four target proteins per membrane, with a stripping step with Stripping Buffer 5X (LI-COR Biosciences, Lincoln, USA) before each reprobing process. For each protein probed, membranes were incubated overnight at room temperature with the primary antibody (1:1000 in Tris Buffered Saline Tween 20, TBS-T) and then with the corresponding secondary IRDye antibody (1:10000 in

TBS-T) for 1 h at room temperature. Primary antibodies used were against β-actin (#3700, Cell Signaling Technology, Danvers, USA) as reference protein; UCP1 (GTX10983, GeneTex, Irvine, USA); MFN2 (HPA030554, Sigma-Aldrich); PPARα (ab8934, Abcam, Cambridge, UK); and against SMAD4 and the phosphorylated (active) and unphosphorylated SMAD2 and SMAD3 proteins, using the SMAD2/3 Antibody Sampler Kit #12747 (Cell Signaling Technology). Protein bands were detected by infrared fluorescence and quantified using an Odyssey near-infrared fluorescence scanner (LI-COR Biosciences). The signal of each protein of interest was normalized to the signal of β-actin or, for the SMAD2/SMAD3 analyses, to nonspecific bands equally abundant in all samples.

2.6 | Histology and immunohistochemistry

Tissue samples were fixed by immersion in 4% paraformaldehyde in 0.1 M sodium phosphate buffer, pH 7.4, overnight at 4°C, dehydrated in a graded series of ethanol, cleared in xylene, and embedded in paraffin blocks for light microscopy. Then, 5-μm-thick sections of tissues were cut with a microtome, mounted on slides, and stained with hematoxylin/eosin. Morphometric analysis of inguinal WAT sections was performed by the digital acquisition of adipose tissue areas using AxioVision 40V 4.6.3.0 software and a Zeiss Axioskop 2 microscope equipped with an AxioCam ICc3 digital camera (Carl Zeiss S.A., Barcelona, Spain). Distributions of adipocyte size were obtained from individual data on cell sizes. Immunohistochemical detection of UCP1 in BAT sections was performed as previously described [32], using a polyclonal antibody against UCP1 (Catalog number GTX112784, GeneTex, Irvine, USA) as the primary antibody.

2.7 | Nonpolar metabolomic analysis

Metabolomic analysis was conducted for six to seven biological replicates (animals) per group on liver, BAT, iWAT, and eWAT samples. Nonpolar metabolites were extracted from 5 mg of lyophilized tissue using methanol: chloroform: 50 mM Tris Buffer (pH 7.5, containing 1 M NaCl) (1:2:1 [v/v]), spiked with 50 mg L^{-1} DL-α-tocopherol acetate as internal standard. After centrifugation (15 min, 14,000 rpm, 4°C), the organic hypophase was transferred into a new vial and dried using the SpeedVac concentrator; finally, samples were resuspended in 100 μl ethyl-acetate and analyzed by liquid chromatography (LC)-atmospheric pressure chemical ionization-mass spectrometry as previously described.[22] For each biological replicate, extractions were performed in triplicate. Full scan MS with data-dependent MS/MS fragmentation and, when available, authentic standards were used for metabolite identification. All solvents and standards used were LC–MS grade quality (CHROMASOLV from Sigma-Aldrich). Metabolites were quantified relatively by normalization on the internal standard (DL-α-tocopherol acetate) amount.

2.8 | Statistical analysis

Data are expressed as mean ± SEM. The statistical significance of differences between groups was assessed by one-way ANOVA, followed by Tukey's Honest Significant Difference post hoc test. The Student's *t* test was used for relevant binary comparisons in specific cases. Analysis was carried out with IBM SPSS Statistics for Windows, Version 27.0. (IMB Corp., New York, USA) and Microsoft Excel (Microsoft, Washington, USA). The threshold of significance was set at $p < 0.05$.

3 | RESULTS

3.1 | DS supplementation attenuated the development of HFD-induced obesity

In our experimental design, obesity-prone mice were pretreated daily for 1 week with DS or its vehicle and then challenged with an obesogenic HFD while continuing to receive the same daily treatments; a third group of animals were fed an NFD and received the vehicle during the whole experimental period. The pretreatment with DS did not affect body weight or body composition as assessed by ECO-MRI, so there were no differences in these parameters among the experimental groups at the start of the 4-week HFD/NFD feeding challenge (data not shown). Body weight gain was higher in the two HFD-fed groups as compared with the NF group from day four of HFD onward, as expected, and lower in the DS group as compared with the HF control group at several experimental time points (Figure 1A) despite higher cumulative energy intake in the DS group (Figure 1B). Expected changes in body composition with HFD feeding—namely, an increase in body fat mass and a decrease in lean body mass expressed as a percentage of body weight—were attenuated in the DS group (Figure 1C,D). Body weight at the experimental endpoint was similarly increased by 7–8% in both groups of mice on the HFD relative to the NF group (Figure 1E). However, the HFD-induced increases in visceral WAT depots mass

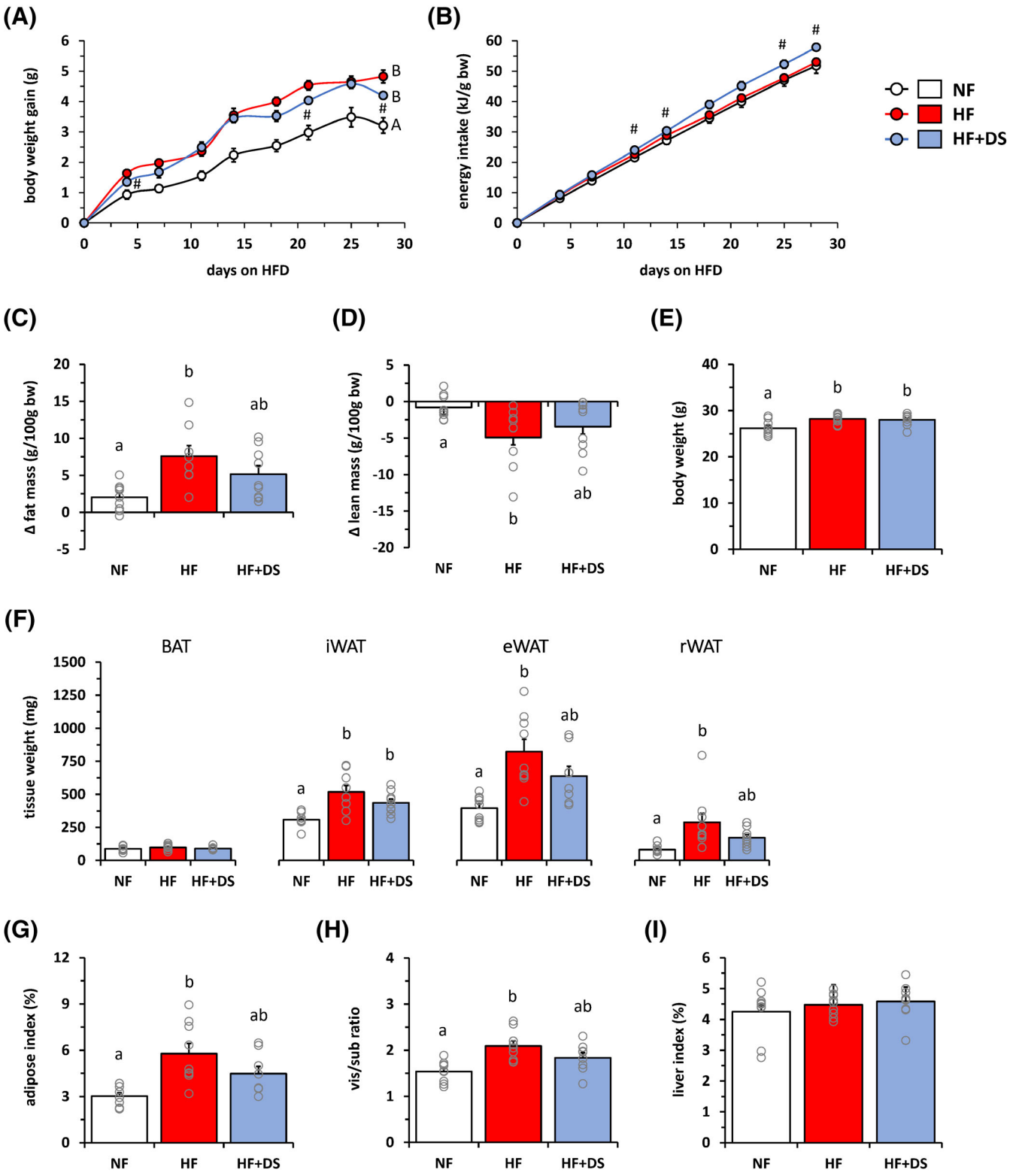

FIGURE 1 Dermatan sulfate (DS) supplementation ameliorated the high-fat diet (HFD)-induced adiposity gain. Obesity-prone mice were challenged with an HFD for 4 weeks while receiving a placebo (HF group) or DS orally (HF + DS group); a third group received a placebo and was kept on a normal-fat diet (NF group). Body weight (bw) gain (A), cumulative energy intake (B), and changes in fat (C) and lean body mass (D) during the dietary challenge. Body weight (E), brown adipose tissue (BAT) and inguinal, epididymal, and retroperitoneal white adipose tissue (iWAT, eWAT, and rWAT) weights (F), adiposity index as the sum of WAT weights as percent bw (G), the visceral (vis: eWAT and rWAT) to subcutaneous (sub: iWAT) ratio (H), and liver index as liver weight as percent bw (I) at the end of the experiment. Data are the means ± SEM of eight to nine animals per group. Repeated measures ANOVA in (A, B) or one-way ANOVA for the other parameters were used to compare between groups. All ANOVA tests were followed by Tukey's Honest Significant Difference post hoc test; bars not sharing letters are significantly different ($p < 0.05$). Single comparisons between the HF + DS and the HF control group were carried out by Student's t test (#, $p < 0.05$).

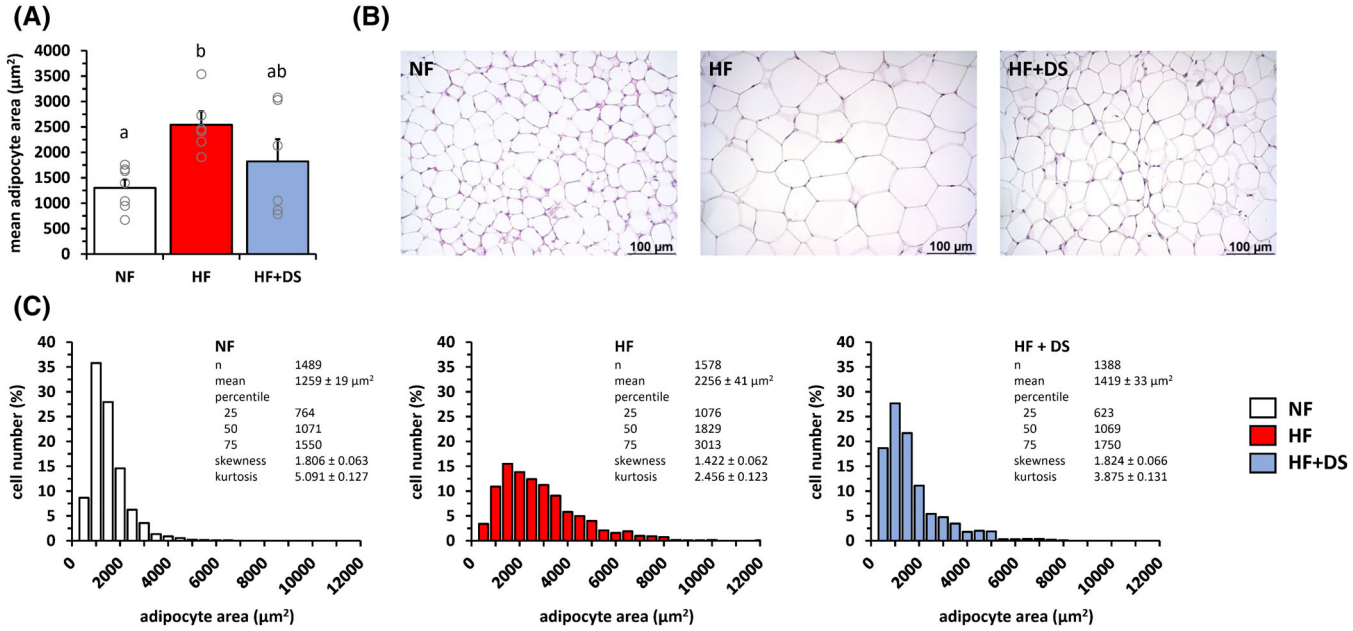

FIGURE 2 Dermatan sulfate (DS) supplementation decreased adipocyte size after the high-fat diet (HFD). Obesity-prone mice were challenged with an HFD for 4 weeks while receiving a placebo (HF group) or DS orally (HF + DS group); a third group received a placebo and was kept on a normal-fat diet (NF group). Mean adipocyte area (A), representative microphotographs illustrating adipocyte size (B), and distribution of adipocyte size (C) in inguinal white adipose tissue at the end of the experiment. Data are the means ± SEM of six to seven animals per group. In (A), to compare between groups, one-way ANOVA followed by Tukey's Honest Significant Difference post hoc test was used: bars not sharing letters are significantly different ($p < 0.05$). In (C), between 200 and 300 cells per animal were included in the analysis. Adipocyte size distribution was statistically different with $p < 0.001$ between groups, according to the Kolmogorov–Smirnov test.

(retroperitoneal and epididymal), overall adiposity index, and visceral to subcutaneous fat ratio were all attenuated in the DS mice as compared with the HF control mice (Figure 1F–H). There were no differences among groups in BAT weight (Figure 1F) and liver index (Figure 1I).

Histological analysis evidenced a marked increase in iWAT mean adipocyte area in the HF control group, which was attenuated in the DS group (Figure 2A,B). Frequency distribution of adipocyte size indicated a lower percentage of small adipocytes and an enrichment in large adipocytes in iWAT of the HF mice as compared with the NF controls (Figure 2C), consistent with a preponderance of adipocyte hypertrophy over hyperplasia after 4 weeks of HFD feeding. Compared with that of HF mice, the iWAT of DS mice was relatively enriched in small adipocytes and depleted of large adipocytes (Figure 2C), suggesting a higher contribution of adipocyte hyperplasia to adipose tissue expansion in the DS-supplemented HFD-fed mice.

3.2 | DS supplementation attenuated HFD-induced alterations in glucose control and insulin sensitivity

Excess fat mass generally associates with insulin resistance and alterations in glucose control. Consistent with the differences in body fat gain, HFD feeding led to increased fasting blood glucose levels in the HF control mice but not the DS-supplemented mice (Figure 3A). Fasting blood insulin levels were similar and nonsignificantly higher in both groups of mice on the HFD relative to the NF controls (Figure 3B). Fasting blood NEFA levels showed no remarkable differences among groups (Figure 3C). Insulin resistance as estimated with the HOMA-IR index was significantly increased in the HF control mice, and the increase was attenuated in the DS-supplemented mice (Figure 3D). Likewise, insulin sensitivity as estimated with the R-QUICKI index was more impaired following HFD feeding in the non-supplemented HF control mice than the DS mice (Figure 3E).

3.3 | DS supplementation enhanced energy expenditure, prevented the "whitening" of BAT, and counteracted changes in the BAT nonpolar metabolome induced by an HFD

The fact that protection against HFD-induced adiposity gain in the DS mice occurred despite increased energy intake pointed to the involvement of metabolic mechanisms. We used body weight loss upon a 6-h fast as a

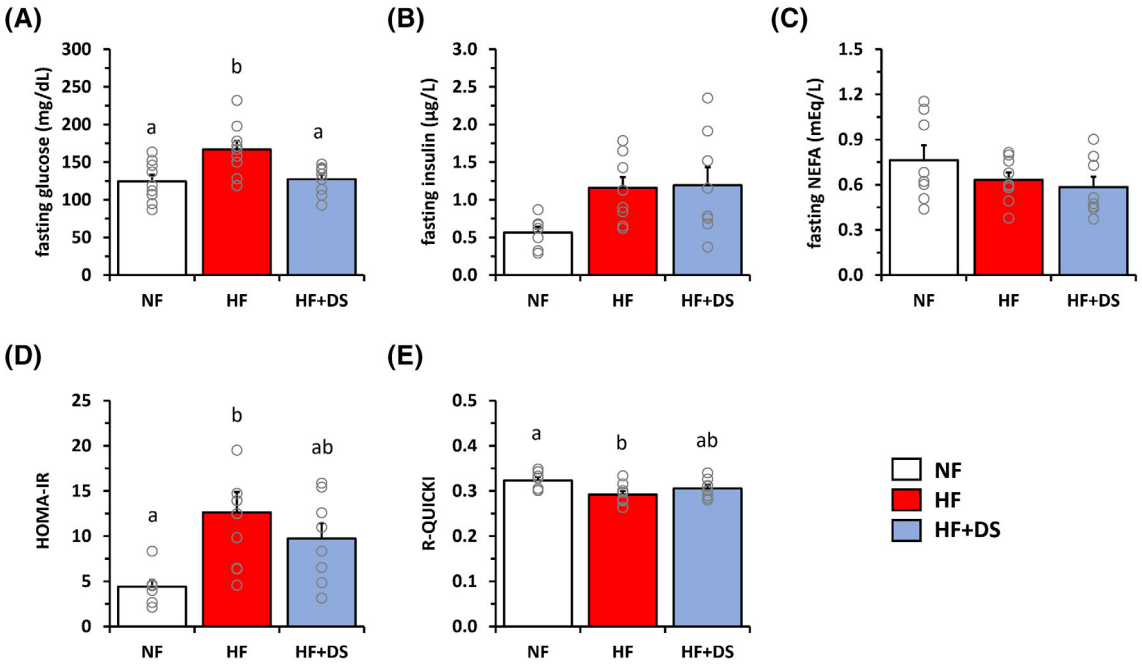

FIGURE 3 Dermatan sulfate (DS) supplementation ameliorated the high-fat diet (HFD)-induced hyperglycemia and insulin resistance. Obesity-prone mice were challenged with an HFD for 4 weeks while receiving a placebo (HF group) or DS orally (HF + DS group); a third group received a placebo and was kept on a normal-fat diet (NF group). Blood glucose (A), serum insulin (B), serum NEFA (C), insulin resistance HOMA-IR (D) index, and insulin sensitivity R-QUICKI (E) index 5–7 days before the sacrifice and after a 6-h fast. Data are the means ± SEM of seven to nine animals per group. To compare between groups, one-way ANOVA followed by Tukey's Honest Significant Difference post hoc test was used: bars not sharing letters are significantly different ($p < 0.05$).

proxy of energy expenditure and found this parameter to be decreased following HFD feeding in the HF control but not the DS mice (Figure 4A). These results strongly suggest that reduced energy expenditure contributes to the development of DIO in the HF control mice and that energy expenditure is higher in the DS mice. Accordingly, DS mice had a higher rectal temperature—another proxy of energy expenditure—than HF mice (measured on the last week of HFD feeding) (Figure 4B).

The above results prompted us to examine the status of WAT browning and BAT activation. Microscopic examination of fixed tissue sections revealed no signs of iWAT browning—such as the presence of brown-like adipose cells with a multilocular intracellular lipid distribution—in any of the experimental groups (see representative images in Figure 2B). No molecular signs of WAT browning were evidenced from gene expression analyses either; even an overall downregulation of genes related to mitochondrial oxidative metabolism and thermogenesis in iWAT and rWAT depots was detected in the HFD-fed groups compared with the NF group (see Section 3.4 and data not shown). On the contrary, in the interscapular BAT depot, HFD feeding induced the expression of UCP1—the key molecular effector of BAT thermogenesis, while other proteins related to mitochondrial oxidative metabolism assayed (PPARα, mitofusin 2) were not downregulated (Figure 4C). Interestingly, UCP1 induction was more consistent and robust in the DS mice than the HF control mice, as shown by immunoblotting (Figure 4C,D) and immunohistochemical staining (Figure 4E). Furthermore, microscopical examination of BAT sections revealed the presence of markedly enlarged intracellular lipid droplets in the brown adipocytes of HF control mice—which is a prominent feature of "whitened" BAT,[13] while DS mice had a more active BAT with smaller, closely packed adipocytes and smaller lipid droplets (Figure 4E).

HFD feeding did not affect BAT mass but changed the BAT metabolome differentially in the HF and DS groups. Metabolomic analysis identified 82 nonpolar species in BAT, of which 25 showed differences in relative accumulation among groups. The HF mice displayed increased relative levels per gram of BAT of all differential lipid metabolites (23 species) compared to the NF mice (Figure 4F, left panel). The altered metabolites included several species of triacylglycerol (TAG) and phospholipids from the group of phosphatidylcholines (PC), three metabolites of arachidonic acid (5-Oxo-ETE, prostacyclin, 11,14,15-theta), and one metabolite of cholesterol (cholestanetriol). Interestingly, the HFD-induced changes in BAT metabolome were markedly attenuated in the DS mice, which only showed increased relative

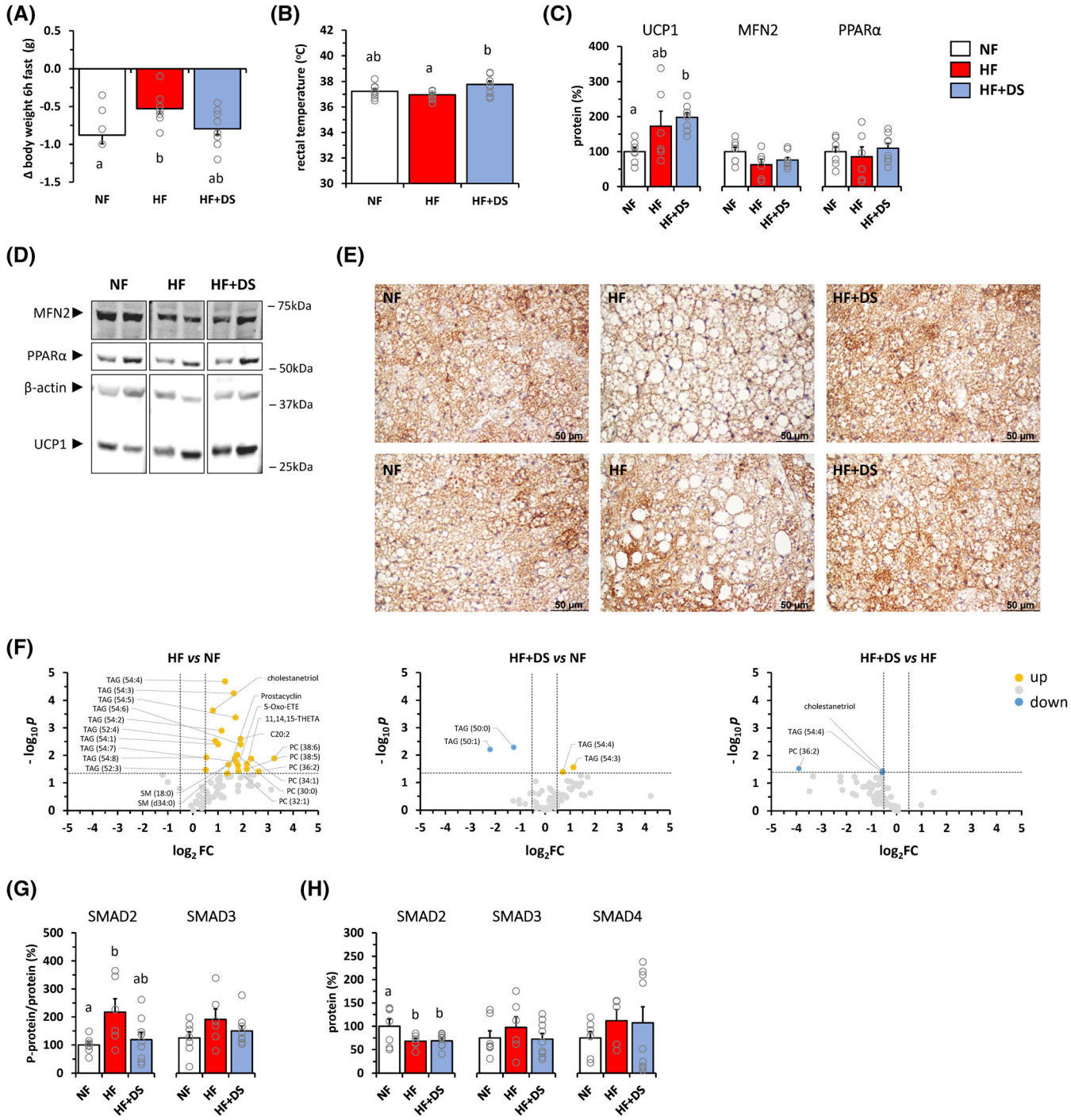

FIGURE 4 Signs of increased energy expenditure and brown adipose tissue (BAT) activation in the dermatan sulfate (DS)-supplemented, high-fat diet (HFD)-fed mice. Obesity-prone mice were challenged with an HFD for 4 weeks while receiving a placebo (HF group) or DS orally (HF + DS group); a third group received a placebo and was kept on a normal-fat diet (NF group). Body weight lost upon a 6-h fast (A) and rectal temperature (B) 5–7 days before the sacrifice. Protein levels (C) and representative immunoblots (D) of the thermogenic/oxidative metabolism indicated genes in BAT, and representative microphotographs of two mice per group illustrating BAT activation and uncoupling protein 1 (UCP1) immunostaining (E) at the end of the experiment. Volcano plots of nonpolar species differentially accumulated in BAT between the indicated groups (F). The ratio of active (phosphorylated) to inactive (unphosphorylated) forms of receptor-regulated SMAD proteins as an indicator of the status of the canonical TGF-β signaling pathway in BAT (G) and protein levels of the indicated SMAD proteins in BAT (H). Data are means ± SEM of six to nine animals per group. Protein expression data are expressed relative to the mean value of the NF control group, which was set to 100. To compare between groups, one-way ANOVA followed by Tukey's Honest Significant Difference post hoc test was used: bars not sharing letters are significantly different ($p < 0.05$). In (F), single comparisons between groups were carried out by Student's *t* test, with the significance threshold at $p < 0.05$. PC, phosphatidylcholine; SM, sphingomyelin; TAG, triacylglycerol.

levels per gram of BAT of two TAG species and even decreased levels of two other TAG species compared with the NF mice (Figure 4F, middle panel). Compared with the HF mice, the DS mice showed significantly decreased relative levels per gram of BAT of cholestanetriol, one PC, and one TAG species (Figure 4F, right panel). The nonpolar metabolome of subcutaneous and visceral WAT depots was less changed qualitatively by HFD feeding (only 2 out of 70 lipid species identified in WAT depots showed differences), and there were no noticeable differences between the HF and DS groups (results not shown).

Transforming growth factor beta (TGF-β) signaling through the SMAD2/3 pathway is inhibitory to BAT recruitment/thermogenesis[23,24] and beige adipogenesis.[25] Further, evidence from a study in DS-treated mice[26] and a genetic mouse model with decreased endogenous tissue DS levels[27] suggests DS may downregulate TGF-β production and activity in tissues. This background prompted us to examine the status of the canonical TGF-β/SMAD 2/3 signaling pathway in BAT in our experiment, for which we used specific monoclonal antibodies against the active (phosphorylated) and inactive (unphosphorylated) forms of the receptor-regulated SMAD2 and SMAD3 proteins. Although with high interindividual variability, the phospho-SMAD2/SMAD2 and, to a lesser extent, phospho-SMAD3/SMAD3 ratios in BAT were lower in the DS mice than the HF mice, whereas levels of SMAD4—the common-partner SMAD protein—were similar in both groups (Figure 4G,H). These results suggest inhibitory TGF-β signaling to BAT thermogenesis is attenuated in the DS mice compared to the HF control mice.

3.4 | DS supplementation modulated metabolic gene expression in visceral WAT and skeletal muscle

HFD feeding provoked changes in the expression of metabolic genes in the visceral (retroperitoneal) WAT depot that, in general, were not affected by DS supplementation. Expression levels in rWAT of genes related to thermogenesis/mitochondrial oxidative metabolism/brown adipocytes (*Ucp1*, *Cidea*, *Ppara*, *Ppargc1a*, *Slc27a1*, *Cpt1b*), the cellular uptake of free fatty acids (*Cd36*), and the mobilization of fatty acids from intracellular TAG stores through lipolysis (*Lipe*, *Pnpla2*) were all lower in the two HFD-fed groups as compared with the NF group (Figure 5A). The expression of specific genes related to the de novo synthesis of fatty acids, namely *Fasn* and (though nonsignificantly) *Scd1*, was also downregulated in both HFD-fed groups (Figure 5B). On the opposite, the expression of *Mest*, a potential marker of WAT expansion under obesogenic conditions,[28] was higher in the two HFD-fed groups (Figure 5C), as expected. Expression levels of *Lpl* and *Srbf1* were similar in all the experimental groups. Out of all the metabolic genes analyzed, only *Slc2a4* (coding the insulin-dependent glucose transporter GLUT4) and *Pparg* (coding the master regulator of adipogenesis and adipose tissue PPARγ) showed differences in expression in rWAT between DS and HF mice. The expression of both genes was lower in the DS mice (Fig, 5B), which could be connected to their reduced expansion of visceral fat depot after the HFD. Additionally, HFD-induced increases in the mRNA levels in rWAT of *Mcp1* (which encodes for monocyte chemoattractant protein-1) and *Cd68* (which encodes for a classical macrophage marker surface protein) were apparent in the HF mice when compared to the NF controls ($p = 0.064$, Student's t test, for *Mcp1*), and attenuated in the DS mice (Figure 5D), possibly related also to their decreased expansion of visceral fat after the HFD.

Skeletal muscle plays a significant role in whole-body glucose homeostasis and is highly responsive to changes in the availability of glucose and fatty acids. DS supplementation strongly impacted the capabilities for substrate uptake, substrate metabolism, and insulin responsiveness in skeletal muscle (Figure 5E). Compared with either the NF or HF mice, the DS-supplemented mice showed dramatically increased muscle expression levels of genes for proteins involved in the cellular provision and uptake of fatty acids (*Lpl*, *Cd36*), the *Ucp3* gene—whose protein product facilitates fatty acid oxidation and minimizes reactive oxygen species production in muscle cells[29]—and genes for proteins in the insulin signaling pathway (*Insr*, coding the insulin receptor, and *Irs1*, coding the insulin receptor substrate). HFD feeding upregulated muscle *Ppargc1a* expression levels in the HF control mice but not the DS mice, and the GLUT4 gene, *Slc2a4*, in both the HF and DS mice, yet more consistently in the latter. The DS mice also displayed lower muscle expression levels of *Ppard* and higher of *Cpt1b* compared with the HF control mice. Other genes assayed (*Mcad*, *Slc2a1*) were similarly expressed in skeletal muscle regardless of the group.

3.5 | DS supplementation modulated liver metabolic and autophagy capabilities, as well as the hepatic nonpolar metabolome

The HFD challenge applied did not result in increased total liver lipid content (Figure 6A), possibly due to its relatively short duration (4 weeks), since chronic HFD feeding for more extended periods (e.g., 18 weeks) causes

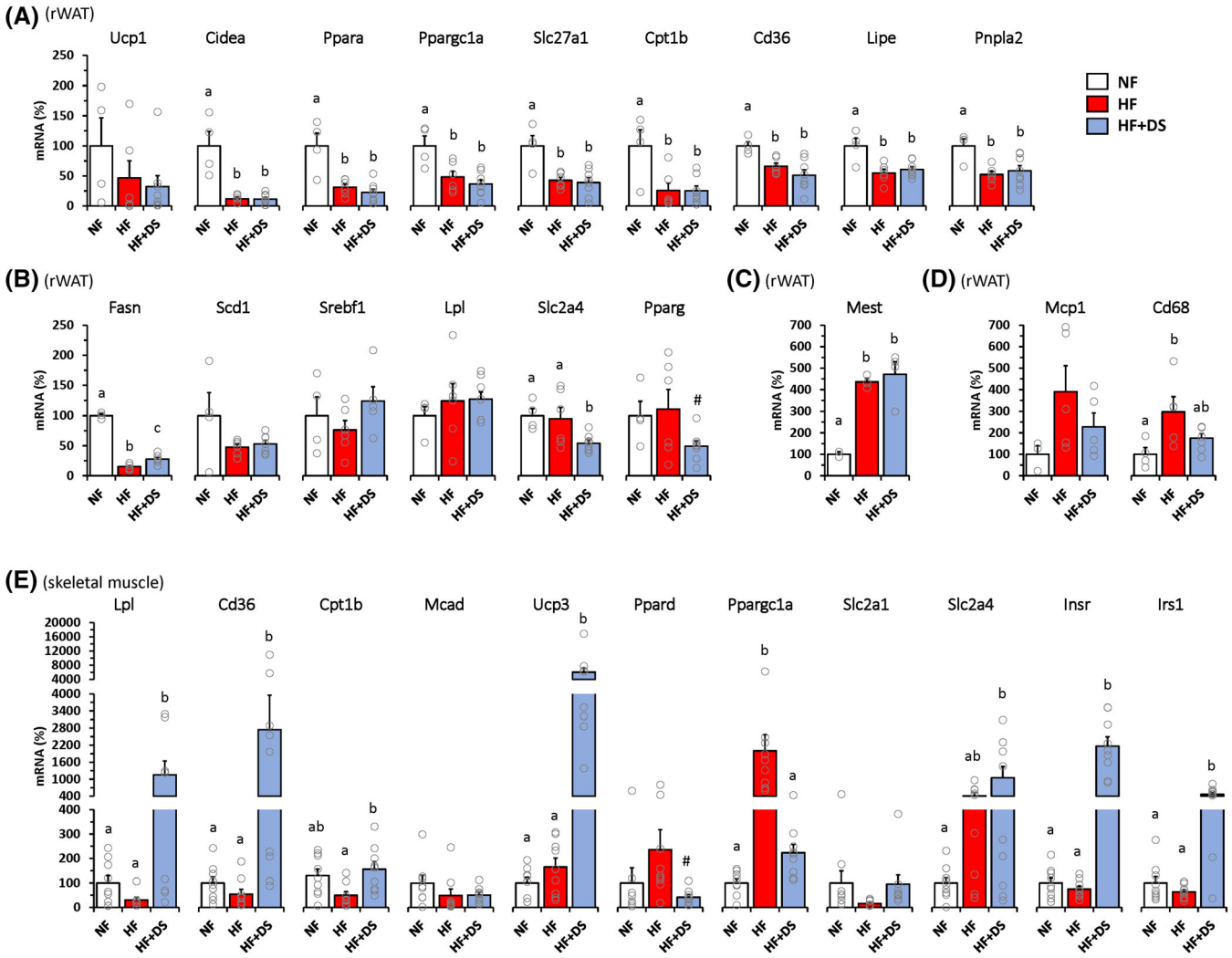

FIGURE 5 mRNA levels of the indicated genes in retroperitoneal white adipose tissue (rWAT) (A-D) and skeletal muscle (E) at the end of the experiment. Obesity-prone mice were challenged with a high-fat diet for 4 weeks while receiving a placebo (HF group) or DS orally (HF + DS group); a third group received a placebo and was kept on a normal-fat diet (NF group). Data are means ± SEM of four to nine animals per group and are expressed relative to the mean value of the NF control group, which was set to 100. To compare between groups, one-way ANOVA followed by Tukey's Honest Significant Difference post hoc test was used: bars not sharing letters are significantly different ($p < 0.05$). Single comparisons between the HF + DS and the HF control group were carried out by Student's *t* test (#, $p < 0.05$).

the accumulation of liver fat in C57BL/6J male mice.[30] Analysis of the hepatic expression of selected genes related to metabolism, autophagy, and inflammation revealed differences among groups (Figure 6B–E). HFD feeding downregulated the hepatic expression of the lipogenesis-related genes *Fasn* and *Scd1* selectively in the DS mice; other lipogenic genes (*Gpat*, *Srebf1*) and oxidative metabolism/fatty acid catabolism-related genes (*Ppara*, *Ppargc1a*, *Cpt1a*) assayed were similarly expressed in all groups (Figure 6B). As to the glucose metabolism-related genes (Figure 6C), the DS mice displayed decreased hepatic expression levels of *Gck*—encoding glucokinase, which can also be considered a lipogenic enzyme,[31,32] and *Pepck*—encoding phosphoenolpyruvate carboxykinase, a limiting enzyme for gluconeogenesis—as compared with the HF control mice. HFD feeding upregulated the hepatic expression of *Map1lc3b*—encoding LC3 protein, central to the autophagy process—in the HF control group but not the DS group and the picture was similar for *Foxo3a* and, though nonsignificant, other autophagy-related genes assayed (*Becn1*, *Atg7*) (Figure 6D). Thus, the hepatic expression of all autophagy-related genes assayed was lower or tended so in the DS mice as compared with the HF mice. Similarly, the hepatic expression of the manganese superoxide dismutase gene (*Sod2*)—which increases upon oxidative stress through ROS-mediated activation of specific transcription factors, such as NF-κB and AP-1[33]—tended

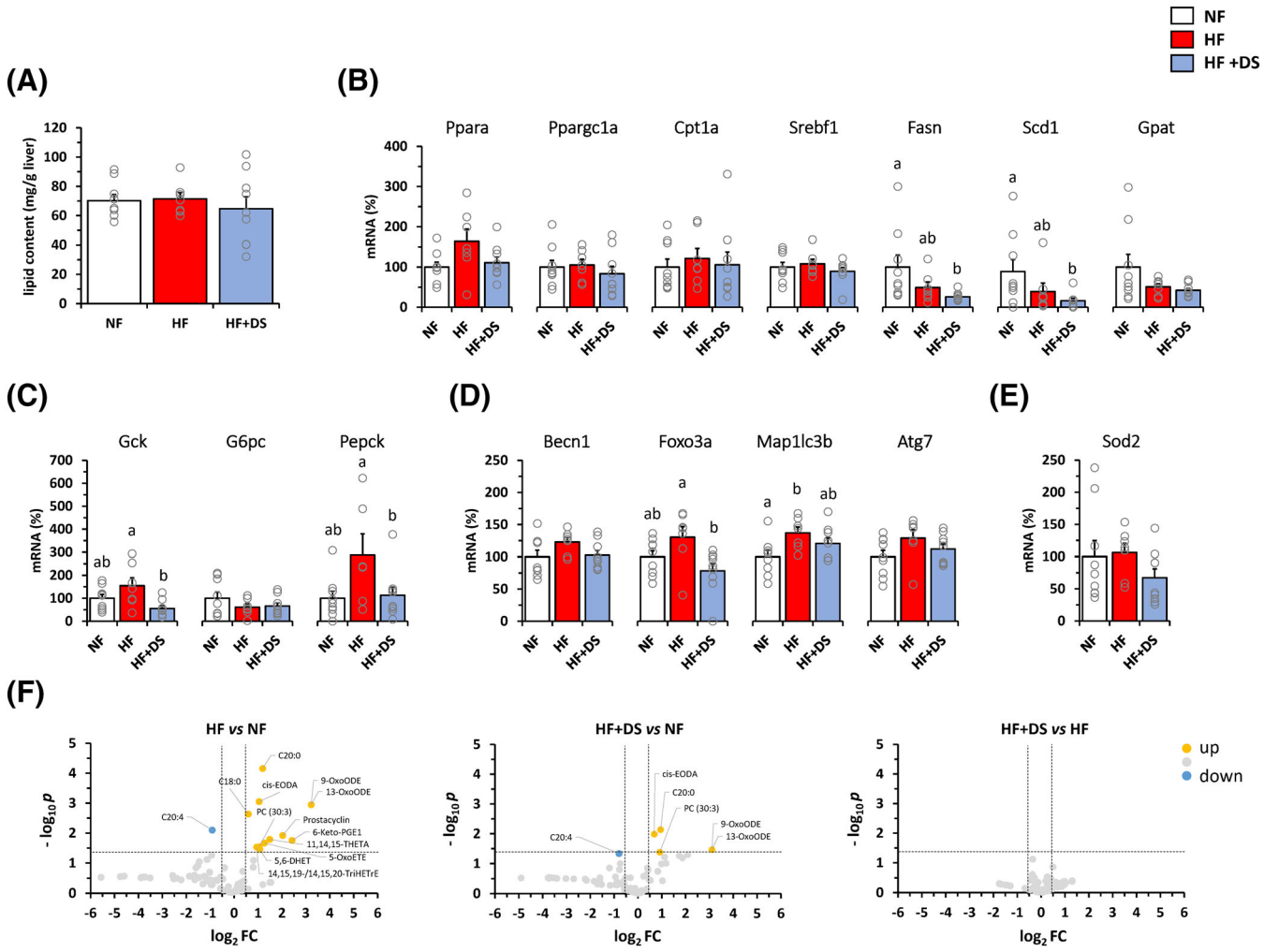

FIGURE 6 Dermatan sulfate (DS) supplementation affected liver parameters after the high-fat diet (HFD). Obesity-prone mice were challenged with an HFD for 4 weeks while receiving a placebo (HF group) or DS orally (HF + DS group); a third group received a placebo and was kept on a normal-fat diet (NF group). Liver total lipid content (A), mRNA levels of the indicated genes in the liver (B, C, D, E), and Volcano plots of lipid species identified in the liver that changed between the indicated groups (F) at the end of the experiment. Data are means ± SEM of six to nine animals per group. mRNA expression data are expressed relative to the mean value of the NF control group, which was set to 100. To compare between groups, one-way ANOVA followed by Tukey's Honest Significant Difference post hoc test was used: bars not sharing letters are significantly different ($p < 0.05$). In (F), single comparisons between groups were carried out by Student's *t* test, with the significance threshold at $p < 0.05$. PC, phosphatidylcholine.

lower in the DS mice ($p = 0.072$, Students *t* test) (Figure 6E), consistent with a lower degree of oxidative stress in these mice as compared with the HF controls.

Metabolomic analyses revealed several differentially accumulated metabolites per gram of liver tissue in the HF mice compared with the NF controls (Figure 6F, left panel). The relative levels of arachidonic acid (C20:4) were decreased, and those of arachidonic acid-derived metabolites (i.e., 5-oxo-ETE; 5,6-DHET; 6-keto PGE1; prostacyclin; 11,14,15-THETA) increased in the liver of HF mice. Interestingly, DS treatment during HFD offset the increases in arachidonic acid-derived metabolites in the liver, including the increases in 5-oxo-ETE, a potent pro-inflammatory 5-lipoxygenase product.[34]

4 | DISCUSSION

In this work, building on previous research from our group,[14,16] we studied the potential of the GAG DS to counteract the development of obesity in a well-established mouse model, namely obesity-prone C57BL6/J mice fed a fat-rich diet. Results indicate that supplementation with DS attenuates the development of DIO, hyperglycemia, insulin resistance, and tissular inflammatory metabolomes in this model by increasing whole-body energy expenditure through the potentiation of BAT activity and the redirection of substrates toward skeletal muscle.

To our knowledge, this is the first study to investigate the anti-obesity activity of DS tested individually in vivo.

In our previous work, supplementation of a DS-containing GAG mix (Oralvisc, hyaluronic acid: DS, 1:0.25) accelerated body fat loss during the reversal of obesity (by changing from an HFD to a regular diet) in DIO mice but failed to counteract the development of DIO in the C57BL6/J model.[16] Those results were obtained at a dose of 3 mg of GAG mix/mouse/d, hence providing 0.75 mg DS, similar to the dose used in the present work (0.8 mg DS/mouse/d). GAG mix supplementation increased the insulin sensitivity of mice under both normal and HFD feeding conditions, yet due to a lowering effect on insulinemia,[16] not on glycemia as found here in the HFD-fed mice supplemented solely with DS. Additionally, GAG mix supplementation did not affect the animals' cumulative energy intake on an HFD,[16] whereas DS supplementation led to increased energy intake on an HFD (this work). Taken together, it is suggested that there are functional interactions between the two Oralvisc GAG mix components in vivo that condition the biological activity of the mix. It is to be noted that interactions were already observed when examining the impact of this mix and its components on the differentiation fate of primary MEFs.[14]

DS mice lost more weight when fasting and had higher rectal temperature than the HF mice, strongly suggesting that their reduced development of DIO is due to increased energy expenditure. The greater energy intake observed in the DS mice is in good concordance, as it may reflect compensatory stimulation of food intake to maintain energy balance in the setting of increased energy expenditure.[35] Interestingly, DS supplementation modified fat depot expansion on an HFD quantitatively, decreasing it and qualitatively, favoring the hyperplasic component of WAT expansion. This is of interest because adipocyte hyperplasia (increase in adipocyte number following recruitment and differentiation of adipose precursor cells), as opposed to hypertrophy (increase in adipocyte size), is thought to be protective from obesity-associated metabolic complications such as insulin resistance and to represent a healthier form of WAT expansion.[36,37] Decreased HFD-induced adipocyte hypertrophy in the DS mice could have led to lower macrophage infiltration in visceral WAT (rWAT) in these mice as compared to the HF controls, as suggested by the consistent *Mcp1* and *Cd68* mRNA expression results. Less macrophage infiltration and, hence, reduced local inflammation could contribute to DS mice's better metabolic parameters after the HFD. Obesity-induced metabolic syndrome is well known to be associated with the acceleration of inflammation via the recruitment of macrophages in adipose tissues.[38]

WAT browning and BAT activation are metabolic mechanisms that can increase whole-body energy expenditure and oppose the development of DIO. No histological or molecular evidence of WAT browning was found in the DS mice. In fact, the HF control and DS mice showed reduced gene expression related to thermogenesis and oxidative metabolism in iWAT after the HFD challenge compared to the NF mice. This adaptation to efficiently store energy in WAT depots has been observed repeatedly in mice during dietary fat excess (revised in Ref. 39). However, the shared WAT metabolic phenotype was associated with signs of decreased whole-body energy expenditure (less weight lost after a 6-h fast) in the HF control mice but not the DS mice. The difference could be explained because the DS mice had a more active BAT after the HFD, as indicated by the tissue's histological appearance and the UCP1 immunoblotting and immunohistochemical staining results. Microscopical examination revealed a hallmark of "whitened" BAT, namely increased intracellular fat deposition, in the HF mice but not the DS mice compared to the NF mice. The metabolomic results aligned with the histological findings by showing a marked increase in the relative levels of various TAG and phospholipid species in BAT of HF mice compared to NF mice that, for most lipid species, was attenuated in the DS animals. "Whitened" brown adipocytes have an enlarged endoplasmic reticulum[40] besides enlarged intracellular lipid droplets, which could explain the phospholipid results. Further, BAT whitening courses with tissue inflammation[13] and our metabolomic results indicated HFD-induced increases in the relative levels of pro-inflammatory lipids such as cholestanetriol and 5-oxo-ETE in BAT of the HF mice, which were suppressed in the DS mice. Cholestanetriol is a pro-inflammatory and proatherogenic oxysterol,[41,42] whereas 5-oxo-ETE is a potent pro-inflammatory 5-lipoxygenase product.[43] Trends to HFD-induced increases in the expression in BAT of genes for pro-inflammatory cytokines such as interleukin 6 and MCP1 were also detected in the HF control mice but not the DS mice, though the expression of these cytokine genes could not be detected in all the samples, and, unlike in rWAT, differences in *Mcp1* expression in BAT were not paralleled by differences in the tissue *Cd68* expression (results not shown). A differential role of MCP1 expression in attracting macrophages in WAT and BAT has been previously suggested.[44] Taken together, it appears that HFD feeding leads to BAT whitening, and DS supplementation attenuates this effect. BAT whitening occurs under various experimental conditions, including obesogenic diet feeding, obesity, aging, and thermoneutrality. It can exacerbate the development of obesity, which has led to increased interest in its study. The precise pathological mechanisms underlying BAT whitening are not fully understood and may differ depending on the triggering

condition.[13] Remarkably, a single day of HFD feeding was shown to cause BAT whitening in mice.[45]

Besides BAT, results herein suggest effects on skeletal muscle metabolism and substrate partitioning between skeletal muscle and visceral WAT may contribute to the anti-obesity activity of DS supplementation. Gene expression results are consistent with higher skeletal muscle insulin responsiveness, fatty acid uptake, and oxidation capabilities in the DS-supplemented HFD-fed mice compared with the HF controls. Lower expression levels of *Ppard* (encoding PPARδ) and *Ppargc1a* (encoding the PPARδ coactivator PGC1α) in the muscle of DS mice may seem at odds with this scenario and with the purported metabolic benefits of DS supplementation. However, activation of PPARδ through oral agonist administration was reported in rats to associate with a worsening, not improvement, of insulin-stimulated glucose uptake in skeletal muscle.[46] Interestingly, our results indicate an enhanced partitioning of glucose toward skeletal muscle (where the preferential fate of glucose is oxidation) than toward visceral fat (where preferential fate is energy storage) in the DS mice. This is suggested by the finding that, following HFD feeding, the DS mice (but not the HF controls) simultaneously showed GLUT4 gene expression induced in the skeletal muscle and repressed in the visceral rWAT depot. In addition, HFD feeding upregulated muscle *Lpl* gene expression selectively in the DS mice, pointing to an increased channeling of HFD-derived fatty acids circulating in TAGs toward skeletal muscle in these mice compared to the HF controls.

Higher insulin responsiveness in skeletal muscle of DS mice as suggested by the upregulated expression of both *Insr* and *Irs1* may result in increased muscle insulin-dependent glucose uptake through GLUT4. This enhanced uptake may be one reason the DS mice have lower fasting blood glucose levels than the HF mice. Decreased gluconeogenesis could also contribute, considering that HFD feeding upregulated hepatic *Pepck* expression in the HF control mice but not the DS mice. Similarly, the hepatic expression of autophagy-related genes appeared upregulated after HFD selectively in the HF mice. A previous report that examined the liver autophagy response to an HFD in rats found that the autophagy flux and the hepatic expression of autophagy-related genes were increased after 2 weeks of HFD but attenuated after 10 weeks.[47] It was suggested that the transient increase could represent an adaptive mechanism to eliminate the fat overload through autophagy, thus avoiding the overproduction of potentially hazardous lipid-degradation intermediates.[47] We speculate that after 4 weeks of HFD, the HF control mice in our study are still at this transient increase in liver autophagy. The lack of this autophagic response in the DS mice could result from their increased substrate oxidative metabolism in BAT and skeletal muscle, making the transient activation of liver autophagy unnecessary. A less pro-inflammatory environment in the liver of DS mice may fit in this scenario and is suggested by lower hepatic *Sod2* expression and levels of arachidonic acid-derived metabolites like 5-oxo-ETE found in the DS mice compared to the HF controls.

Although eventual effects on intestinal fat absorption or spontaneous physical activity cannot be ruled out, results in this work indicate that metabolic mechanisms underlie the anti-obesity action of DS. The ultimate explanation for the metabolic effects of DS supplementation remains to be determined. Human studies showed that radiolabeled DS is absorbed following oral administration, especially a subfraction comprising the smaller or less sulfated molecules.[48] Intestinal absorption has been demonstrated for other GAGs, such as hyaluronic acid, following oral administration to rats and dogs.[49] Therefore, it is possible that the DS molecules supplemented, or fragments of them, reach and integrate into the ECM of vascular walls and metabolically relevant tissues. This may lead to remodeling of the ECM, causing alterations in signal processing and the response of parenchymal and precursor cells to autocrine, paracrine, and endocrine signals, ultimately affecting cell fate and metabolism. DS or DS fragments could also function by interacting with specific cell surface receptors.[50,51] The ECM impacts adipogenesis, adipocyte metabolism,[52] and muscle metabolism,[53] with implications for obesity and metabolic diseases. Indeed, genetic rodent models targeting enzymes involved in GAG chain building or proteoglycan core proteins exhibit distinct adipose phenotypes (reviewed in Ref. 3). Finally, it cannot be discarded that changes in the gut microbiota partly mediate the effects of oral-supplemented DS.[54,55] More specifically, our results indicated possible modulatory effects of oral DS supplementation under an HFD on the TGF-β/SMAD 2/3 signaling pathway in BAT. Additionally, increased DS content in the vascular and tissue ECM after oral DS supplementation could result in increased activity of heparin cofactor II (HCII)—a serine protease inhibitor that inactivates thrombin upon complex formation with DS.[56] Evidence in both humans and rodents indicates that HCII exerts positive effects on glucose metabolism and insulin sensitivity via its antithrombotic activity or acting on additional, still unknown, targets.[57,58] Strikingly, decreased HCII genetic charge resulted in increased *Mcp1* gene expression in visceral WAT and increased gluconeogenic *Pepck* gene expression in the liver of HFD-fed heterozygous ($HCII^{+/-}$) mice,[58] which is the opposite of what we found here in the HFD-fed, DS supplemented mice. Thus, the involvement of changes in HCII activity in the positive metabolic effects of DS supplementation in the context of an HFD is suggested.

In conclusion, this work shows that oral DS supplementation counteracts the development of HFD-induced obesity and insulin resistance in obesity-prone mice due, at least in part, to metabolic mechanisms that promote energy expenditure, namely the potentiation of BAT activity through decreased whitening and the redirection of substrates toward skeletal muscle. DS supplementation also resulted in lower levels of pro-inflammatory lipid species in BAT and the liver on an HFD. The results sustain potential uses of DS for the management of body fat and metabolic health, including the prevention and amelioration of BAT whitening, weight gain, and insulin resistance related to obesity and aging.

AUTHOR CONTRIBUTIONS

Bojan Stojnić: Investigation, formal analysis. Sebastiá Galmés: Investigation, formal analysis. Alba Serrano: Investigation. Maria Sulli: Investigation. Lana Sušak: Investigation. Ndioba Seye: Investigation. Andreu Palou: Funding acquisition, writing—review and Editing. Gianfranco Diretto: Methodology, supervision, writing—review and editing. M. Luisa Bonet: Conceptualization, methodology, supervision, writing-original draft. Joan Ribot: Conceptualization, methodology, supervision, formal analysis, data curation, visualization, writing—review and editing.

FUNDING INFORMATION

This work was supported by the Spanish Government (MICIU, AEI, Fondo FEDER/EU) under PGC2018-097436-B-I00 (to A.P.) and AGL2015-67019-P (to A.P.). The authors thank Enzo Ceresi for his help with histology studies and Bioiberica (Palafolls, Barcelona, Spain) for the generous gift of dermatan sulfate.

CONFLICT OF INTEREST STATEMENT

The authors declare no conflicts of interest.

DATA AVAILABILITY STATEMENT

If any researcher wishes, the data are available.

ORCID

Sebastiá Galmés https://orcid.org/0000-0002-4243-9527
Andreu Palou https://orcid.org/0000-0002-0295-4452
Gianfranco Diretto https://orcid.org/0000-0002-1441-0233
M. Luisa Bonet https://orcid.org/0000-0002-8698-0630
Joan Ribot https://orcid.org/0000-0003-4460-9371

REFERENCES

1. Cilla A, Olivares M, Laparra JM. Glycosaminoglycans from animal tissue foods and gut health. Food Rev Intl. 2013;29:192–200.
2. Gandhi NS, Mancera RL. The structure of glycosaminoglycans and their interactions with proteins. Chem Biol Drug des. 2008;72:455–82.
3. Pessentheiner AR, Ducasa GM, Gordts P. Proteoglycans in obesity-associated metabolic dysfunction and meta-inflammation. Front Immunol. 2020;11:769.
4. Gulati K, Poluri KM. Mechanistic and therapeutic overview of glycosaminoglycans: the unsung heroes of biomolecular signaling. Glycoconj J. 2016;33:1–17.
5. Han LK, Sumiyoshi M, Takeda T, Chihara H, Nishikiori T, Tsujita T, et al. Inhibitory effects of chondroitin sulfate prepared from salmon nasal cartilage on fat storage in mice fed a high-fat diet. Int J Obes Relat Metab Disord. 2000;24:1131–8.
6. Hu SW, Tian YY, Chang YG, Li ZJ, Xue CH, Wang YM. Fucosylated chondroitin sulfate from sea cucumber improves glucose metabolism and activates insulin signaling in the liver of insulin-resistant mice. J Med Food. 2014;17:749–57.
7. Hirose S, Asano K, Harada S, Takahashi T, Kondou E, Ito K, et al. Effects of salmon cartilage proteoglycan on obesity in mice fed with a high-fat diet. Food Sci Nutr. 2022;10:577–83.
8. Ahn MY, Hwang JS, Kim MJ, Park KK. Antilipidemic effects and gene expression profiling of the glycosaminoglycans from cricket in rats on a high fat diet. Arch Pharm Res. 2016;39:926–36.
9. Ahn MY, Kim BJ, Kim HJ, Yoon HJ, Jee SD, Hwang JS, et al. Anti-obesity effect of *Bombus ignitus* queen glycosaminoglycans in rats on a high-fat diet. Int J Mol Sci. 2017;18:681.
10. Geetha V, Das M, Zarei M, Vp M, Harohally NV, Suresh Kumar G. Studies on the partial characterization of extracted glycosaminoglycans from fish waste and its potentiality in modulating obesity through in-vitro and in-vivo. Glycoconj J. 2022;39:525–42.
11. Bonet ML, Mercader J, Palou A. A nutritional perspective on UCP1-dependent thermogenesis. Biochimie. 2017;134:99–117.
12. Shimizu I, Walsh K. The whitening of brown fat and its implications for weight management in obesity. Curr Obes Rep. 2015;4:224–9.
13. Ziqubu K, Dludla PV, Mthembu SXH, Nkambule BB, Mabhida SE, Jack BU, et al. An insight into brown/beige adipose tissue whitening, a metabolic complication of obesity with the multifactorial origin. Front Endocrinol. 2023;14:1114767.
14. Petrov PD, Granados N, Chetrit C, Martinez-Puig D, Palou A, Bonet ML. Synergistic effects of a mixture of glycosaminoglycans to inhibit adipogenesis and enhance chondrocyte features in multipotent cells. Cell Physiol Biochem. 2015;37:1792–806.
15. Rai C, Nandini CD, Priyadarshini P. Composition and structure elucidation of bovine milk glycosaminoglycans and their anti-adipogenic activity via modulation PPAR-gamma and C/EBP-alpha. Int J Biol Macromol. 2021;193:137–44.
16. Reynes B, Serrano A, Petrov P, Ribot J, Chetrit C, Martinez-Puig D, et al. Anti-obesity and insulin-sensitising effects of a glycosaminoglycan mix. J Func Foods. 2016;26:350–62.
17. Matthews DR, Hosker JP, Rudenski AS, Naylor BA, Treacher DF, Turner RC. Homeostasis model assessment: insulin resistance and beta-cell function from fasting plasma glucose and insulin concentrations in man. Diabetologia. 1985;28:412–9.
18. Perseghin G, Caumo A, Caloni M, Testolin G, Luzi L. Incorporation of the fasting plasma FFA concentration into QUICKI

improves its association with insulin sensitivity in nonobese individuals. J Clin Endocrinol Metab. 2001;86:4776–81.
19. Serrano A, Ribot J, Palou A, Bonet ML. Long-term programming of skeletal muscle and liver lipid and energy metabolism by resveratrol supplementation to suckling mice. J Nutr Biochem. 2021;95:108770.
20. Petrov PD, Ribot J, Palou A, Bonet ML. Improved metabolic regulation is associated with retinoblastoma protein gene haploinsufficiency in mice. Am J Physiol Endocrinol Metab. 2015; 308:E172–83.
21. Stojnic B, Serrano A, Susak L, Palou A, Bonet ML, Ribot J. Protective effects of individual and combined low dose Beta-carotene and metformin treatments against high-fat diet-induced responses in mice. Nutrients. 2021;13:3607.
22. Sulli M, Mandolino G, Sturaro M, Onofri C, Diretto G, Parisi B, et al. Molecular and biochemical characterization of a potato collection with contrasting tuber carotenoid content. PloS One. 2017;12:e0184143.
23. Lee MJ. Transforming growth factor beta superfamily regulation of adipose tissue biology in obesity. Biochim Biophys Acta Mol Basis Dis (BBA)—Mol Basis Dis. 2018;1864:1160–71.
24. Pervin S, Reddy ST, Singh R. Novel roles of follistatin/myostatin in transforming growth factor-beta signaling and adipose browning: potential for therapeutic intervention in obesity related metabolic disorders. Front Endocrinol. 2021;12:653179.
25. Higa R, Hanada T, Teranishi H, Miki D, Seo K, Hada K, et al. CD105 maintains the thermogenic program of beige adipocytes by regulating Smad2 signaling. Mol Cell Endocrinol. 2018;474: 184–93.
26. Belmiro CL, Goncalves RG, Kozlowski EO, Werneck AF, Takyia CM, Leite M Jr, et al. Dermatan sulfate reduces monocyte chemoattractant protein 1 and TGF-beta production, as well as macrophage recruitment and myofibroblast accumulation in mice with unilateral ureteral obstruction. Braz J Med Biol Res. 2011;44:624–33.
27. Chan WL, Steiner M, Witkos T, Egerer J, Busse B, Mizumoto S, et al. Impaired proteoglycan glycosylation, elevated TGF-beta signaling, and abnormal osteoblast differentiation as the basis for bone fragility in a mouse model for gerodermia osteodysplastica. PLoS Genet. 2018;14:e1007242.
28. Voigt A, Ribot J, Sabater AG, Palou A, Bonet ML, Klaus S. Identification of Mest/Peg1 gene expression as a predictive biomarker of adipose tissue expansion sensitive to dietary anti-obesity interventions. Genes Nutr. 2015;10:477.
29. MacLellan JD, Gerrits MF, Gowing A, Smith PJ, Wheeler MB, Harper ME. Physiological increases in uncoupling protein 3 augment fatty acid oxidation and decrease reactive oxygen species production without uncoupling respiration in muscle cells. Diabetes. 2005;54:2343–50.
30. Mercader J, Ribot J, Murano I, Feddersen S, Cinti S, Madsen L, et al. Haploinsufficiency of the retinoblastoma protein gene reduces diet-induced obesity, insulin resistance, and hepatosteatosis in mice. Am J Physiol Endocrinol Metab. 2009;297: E184–93.
31. Dentin R, Pegorier JP, Benhamed F, Foufelle F, Ferre P, Fauveau V, et al. Hepatic glucokinase is required for the synergistic action of ChREBP and SREBP-1c on glycolytic and lipogenic gene expression. J Biol Chem. 2004;279:20314–26.
32. Peter A, Stefan N, Cegan A, Walenta M, Wagner S, Konigsrainer A, et al. Hepatic glucokinase expression is associated with lipogenesis and fatty liver in humans. J Clin Endocrinol Metab. 2011;96:E1126–30.
33. Kim HP, Roe JH, Chock PB, Yim MB. Transcriptional activation of the human manganese superoxide dismutase gene mediated by tetradecanoylphorbol acetate. J Biol Chem. 1999; 274:37455–60.
34. Grant GE, Rokach J, Powell WS. 5-Oxo-ETE and the OXE receptor. Prostaglandins Other Lipid Mediat. 2009;89:98–104.
35. Bosy-Westphal A, Hagele FA, Muller MJ. What is the impact of energy expenditure on energy intake? Nutrients. 2021;13:3508.
36. Hepler C, Gupta RK. The expanding problem of adipose depot remodeling and postnatal adipocyte progenitor recruitment. Mol Cell Endocrinol. 2017;445:95–108.
37. Longo M, Zatterale F, Naderi J, Parrillo L, Formisano P, Raciti GA, et al. Adipose tissue dysfunction as determinant of obesity-associated metabolic complications. Int J Mol Sci. 2019; 20:2358.
38. Wu H, Ballantyne CM. Metabolic inflammation and insulin resistance in obesity. Circ Res. 2020;126:1549–64.
39. Fromme T, Klingenspor M. Uncoupling protein 1 expression and high-fat diets. Am J Physiol Regul Integr Comp Physiol. 2011;300:R1–8.
40. Kotzbeck P, Giordano A, Mondini E, Murano I, Severi I, Venema W, et al. Brown adipose tissue whitening leads to brown adipocyte death and adipose tissue inflammation. J Lipid Res. 2018;59:784–94.
41. Hubbard RW, Ono Y, Sanchez A. Atherogenic effect of oxidized products of cholesterol. Prog Food Nutr Sci. 1989;13: 17–44.
42. Jusakul A, Yongvanit P, Loilome W, Namwat N, Kuver R. Mechanisms of oxysterol-induced carcinogenesis. Lipids Health Dis. 2011;10:44.
43. Powell WS, Rokach J. In: Steinhilber DE, editor. Lipoxygenases in inflammation progress in inflammation research. Cham: Springer; 2016.
44. Kamei N, Tobe K, Suzuki R, Ohsugi M, Watanabe T, Kubota N, et al. Overexpression of monocyte chemoattractant protein-1 in adipose tissues causes macrophage recruitment and insulin resistance. J Biol Chem. 2006;281:26602–14.
45. Kuipers EN, Held NM, In Het Panhuis W, Modder M, Ruppert PMM, Kersten S, et al. A single day of high-fat diet feeding induces lipid accumulation and insulin resistance in brown adipose tissue in mice. Am J Physiol Endocrinol Metab. 2019;317:E820–30.
46. Cresser J, Bonen A, Chabowski A, Stefanyk LE, Gulli R, Ritchie I, et al. Oral administration of a PPAR-delta agonist to rodents worsens, not improves, maximal insulin-stimulated glucose transport in skeletal muscle of different fibers. Am J Physiol Regul Integr Comp Physiol. 2010;299:R470–9.
47. Papackova Z, Dankova H, Palenickova E, Kazdova L, Cahova M. Effect of short- and long-term high-fat feeding on autophagy flux and lysosomal activity in rat liver. Physiol Res. 2012;61:S67–76.
48. Dawes J, Hodson BA, Pepper DS. The absorption, clearance and metabolic fate of dermatan sulphate administered to man—studies using a radioiodinated derivative. Thromb Haemost. 1989;62:945–9.

49. Balogh L, Polyak A, Mathe D, Kiraly R, Thuroczy J, Terez M, et al. Absorption, uptake and tissue affinity of high-molecular-weight hyaluronan after oral administration in rats and dogs. J Agric Food Chem. 2008;56:10582–93.
50. Mizumoto S, Yamada S, Sugahara K. Molecular interactions between chondroitin-dermatan sulfate and growth factors/receptors/matrix proteins. Curr Opin Struct Biol. 2015;34:35–42.
51. Zhang B, Chi L. Chondroitin sulfate/dermatan sulfate-protein interactions and their biological functions in human diseases: implications and analytical tools. Front Cell Dev Biol. 2021;9:693563.
52. Ruiz-Ojeda FJ, Mendez-Gutierrez A, Aguilera CM, Plaza-Diaz J. Extracellular matrix remodeling of adipose tissue in obesity and metabolic diseases. Int J Mol Sci. 2019;20:4888.
53. Ahmad K, Choi I, Lee YH. Implications of skeletal muscle extracellular matrix remodeling in metabolic disorders: diabetes perspective. Int J Mol Sci. 2020;21:3845.
54. Shang Q, Shi J, Song G, Zhang M, Cai C, Hao J, et al. Structural modulation of gut microbiota by chondroitin sulfate and its oligosaccharide. Int J Biol Macromol. 2016;89:489–98.
55. Rawat PS, Seyed Hameed AS, Meng X, Liu W. Utilization of glycosaminoglycans by the human gut microbiota: participating bacteria and their enzymatic machineries. Gut Microbes. 2022;14:2068367.
56. Tollefsen DM. Vascular dermatan sulfate and heparin cofactor II. Prog Mol Biol Transl Sci. 2010;93:351–72.
57. Hasegawa Y, Ishigaki Y. Heparin cofactor II: a novel plausible link of obesity and diabetes with thrombosis. J Atheroscler Thromb. 2017;24:1202–3.
58. Kurahashi K, Inoue S, Yoshida S, Ikeda Y, Morimoto K, Uemoto R, et al. The role of heparin cofactor II in the regulation of insulin sensitivity and maintenance of glucose homeostasis in humans and mice. J Atheroscler Thromb. 2017;24:1215–30.

How to cite this article: Stojnić B, Galmés S, Serrano A, Sulli M, Sušak L, Seye N, et al. Glycosaminoglycan dermatan sulfate supplementation decreases diet-induced obesity and metabolic dysfunction in mice. BioFactors. 2023. https://doi.org/10.1002/biof.2022